

Article

Design and Optimization of Compact Printed Log-Periodic Dipole Array Antennas with Extended Low-Frequency Response

Keyur K. Mistry ¹, Pavlos I. Lazaridis ^{2,*} , Zaharias D. Zaharis ³  and Tian Hong Loh ⁴ ¹ Oxford Space Systems, Harwell OX11 0RL, UK; keyur.mistry@oxford.space² Department of Engineering and Technology, University of Huddersfield, Huddersfield HD1 3DH, UK³ Department of Electrical and Computer Engineering, Aristotle University of Thessaloniki, 54124 Thessaloniki, Greece; zaharis@auth.gr⁴ 5G and Future Communications Technology Group, National Physical Laboratory, Teddington TW11 0LW, UK; tian.loh@npl.co.uk

* Correspondence: p.lazaridis@hud.ac.uk

Abstract: This paper initially presents an overview of different miniaturization techniques used for size reduction of printed log-periodic dipole array (PLPDA) antennas, and then continues by presenting a design of a conventional PLPDA design that operates from 0.7–8 GHz and achieves a realized gain of around 5.5 dBi in most of its bandwidth. This antenna design is then used as a baseline model to implement a novel technique to extend the low-frequency response. This is completed by replacing the longest straight dipole with a triangular-shaped dipole and by optimizing the four longest dipoles of the antenna using the Trust Region Framework algorithm in CST. The improved antenna with extended low-frequency response operates from 0.4 GHz to 8 GHz with a slightly reduced gain at the lower frequencies.

Keywords: CST simulations; printed log-periodic dipole array antennas; UWB antennas



Citation: Mistry, K.K.; Lazaridis, P.I.; Zaharis, Z.D.; Loh, T.H. Design and Optimization of Compact Printed Log-Periodic Dipole Array Antennas with Extended Low-Frequency Response. *Electronics* **2021**, *10*, 2044. <https://doi.org/10.3390/electronics10172044>

Academic Editors: Giovanni Andrea Casula and Dimitra I. Kaklamani

Received: 16 July 2021

Accepted: 19 August 2021

Published: 24 August 2021

Publisher's Note: MDPI stays neutral with regard to jurisdictional claims in published maps and institutional affiliations.



Copyright: © 2021 by the authors. Licensee MDPI, Basel, Switzerland. This article is an open access article distributed under the terms and conditions of the Creative Commons Attribution (CC BY) license (<https://creativecommons.org/licenses/by/4.0/>).

1. Introduction

With the rapid technological advancements over the last decade, there is an increased demand for new generation wireless devices and communication systems. An ultra-wideband (UWB) frequency range from 3.1 GHz to 10.6 GHz is legislated by the Federal Communication Commission (FCC) for use with wireless communication systems [1,2]. Most of the UWB systems require antennas with large bandwidth. Several researchers propose utilizing monopole antennas for this application [3–5]. However, although some monopole antennas can have wide bandwidth, they do not provide fixed radiation patterns for their entire frequency range, and thus alternative antennas for this application are required. Vivaldi antennas, also known as tapered slot antennas, are also considered good candidates for UWB applications because of their stable radiation pattern over their operating frequency range and their ability to radiate or receive power in the end-fire direction [6–8]. However, the size of these antennas can be large, depending on the lowest operating frequency. Therefore, for such applications, wideband LPDAs (Log-Periodic Dipole Arrays) are highly preferred because they are directive and provide flat gain, wide bandwidth, and can be fabricated at a low cost [9–11]. Moreover, they radiate in the end-fire direction and also provide closely spaced multiple resonances in the operating frequency range.

Additionally, wideband directive antennas are also in huge demand by industrial as well as military organizations for direction-finding (DF) applications over a wide frequency range. Such applications require directive wideband antennas to determine the angle of the originating signal source in the azimuth plane as well as to have the ability to receive the signal over a wide frequency range [12,13]. Moreover, DF techniques are also used for

several civilian applications to track and locate targets. A fixed surveillance system requires a DF antenna in the form of an array consisting of multiple antenna elements that are arranged in a circular formation. The antenna elements can be among several antenna types such as dipole antennas, monopole antennas, bi-conical antennas, log-periodic antennas, and Vivaldi antennas. A portable wideband DF antenna is proposed in [12,14]. DF antennas have also found application in the drone market, where these antenna systems are deployed on vehicles as studied in [15,16]. LPDAs are extensively used for DF applications because of their highly directive radiation pattern resulting in an adequate front-to-back ratio in a wide range of frequencies [16]. However, the size of LPDAs can be large, and thus there is a case for size reduction in order for them to be deployed, e.g., on drones.

Antennas are also used in anechoic and reverberation chambers for Electromagnetic Compatibility (EMC) measurements, where they are used as a source of electromagnetic radiation. Such type of measurement requires the source antenna to be of small size with wideband characteristics [15]. LPDAs are also considered as one of the best candidates for this application.

The concept of frequency-independent antennas was first proposed by Rumsey in [17]. The study conducted by Rumsey provided the foundation for the invention of the LPDA in later years, as suggested in [18]. The design procedure for a conventional LPDA was suggested by Isbell and Carrel [16,19–21]. Due to the fact that LPDAs can operate in a wide frequency range and provide flat gain and highly directive radiation patterns, they are a promising candidate for applications such as UWB communication systems, DF, EMC, and radars.

However, for some of the above-mentioned applications, the size of the antenna should be reasonably small. This puts a limitation on the use of LPDAs, because for the lower frequencies, the size of some dipole elements is large, and thus there is a demand for smaller alternative antennas. In pursuit of reducing the size of LPDAs, several studies were carried out by designing microstrip-printed LPDAs (PLPDAs) [22–24]. The advantages of designing PLPDAs are miniaturization and low-fabrication cost. This paper investigates several miniaturization techniques that have been proposed by researchers and additionally proposes a novel design of an extended low-frequency response PLPDA that operates from 0.4 GHz to 8 GHz.

2. Miniaturization Techniques for Size-Reduction of PLPDAs

Several studies have been carried out, and several techniques have been proposed to reduce the size of PLPDAs. This section investigates various miniaturization techniques proposed by researchers to reduce the size of PLPDAs.

2.1. Top-Loading Techniques

The top-loading techniques involve the addition of different shapes of elements, such as T-shaped, double T-shaped, hat-shaped, arc-shaped, C-shaped, or any other shaped element at the termination of the dipoles of the conventional PLPDA. However, while adding the top-loading element at the termination of the dipole, the physical length of the dipole should be the same as that previously.

T-top loaded elements and hat-top loaded elements have been proposed and implemented in [25] to design a 48-dipole PLPDA which operates in the frequency range from 0.55 GHz to 9 GHz, providing a realized gain of above 7 dBi in the operating frequency range. A convention 48-dipole PLPDA was initially designed with a scaling factor (τ) of 0.935 and a spacing factor (σ) of 0.174 in order to achieve a directivity of 9.5 dBi. However, in an attempt to reduce the length of the overall antenna, the spacing factor was reduced from 0.174 to 0.06 in order to achieve a 20% size reduction of the boom length of the antenna, thereby reducing the resulting PLPDA length from 321 mm to 268 mm. Additionally, in order to reduce the overall width of the antenna, T-top loaded elements and hat-top loaded elements were introduced at the ends of the last six longer dipoles. This technique has reduced the overall width of the antenna by 27%. The overall size of 268 mm \times 194 mm

(length \times width) of the antenna was achieved after implementing this technique. The study presented in this paper also demonstrates that for the same physical length, the resonance at the lowest operating frequency of the straight monopole can be lowered by using T-top loading elements. The resonance in the lower frequency band obtained by introducing T-top loaded elements can be further lowered by introducing vertical parts to make it a hat-top loaded element. A simple analysis to support this technique was demonstrated in [25] by designing a straight monopole that resonates at 1 GHz. After the introduction of a T-top loaded element and a hat-top loaded element to the straight monopole, the resonance shifted from 1 GHz to 0.8 GHz and 0.7 GHz, respectively. Therefore, a 35% size reduction was obtained by introducing a hat-top loaded element instead of using a straight monopole to obtain resonance at 0.7 GHz. However, the limitation of such loading techniques is that it becomes difficult to attain the maximum impedance bandwidth because of the relatively higher Q-factor. Due to this reason, there is a need for bandwidth enhancement techniques to be introduced in the miniaturized version of the PLPDA. Again, in [25], bandwidth enhancement for the miniaturized PLPDA is obtained by introducing a feedline meander, a trapezoidal resistive stub for the modified dipoles, and an arrow-shaped balun near the feeding of the antenna. Figure 1 shows a schematic diagram of the implemented hat-loading as well as T-loading techniques to a PLPDA in [25].

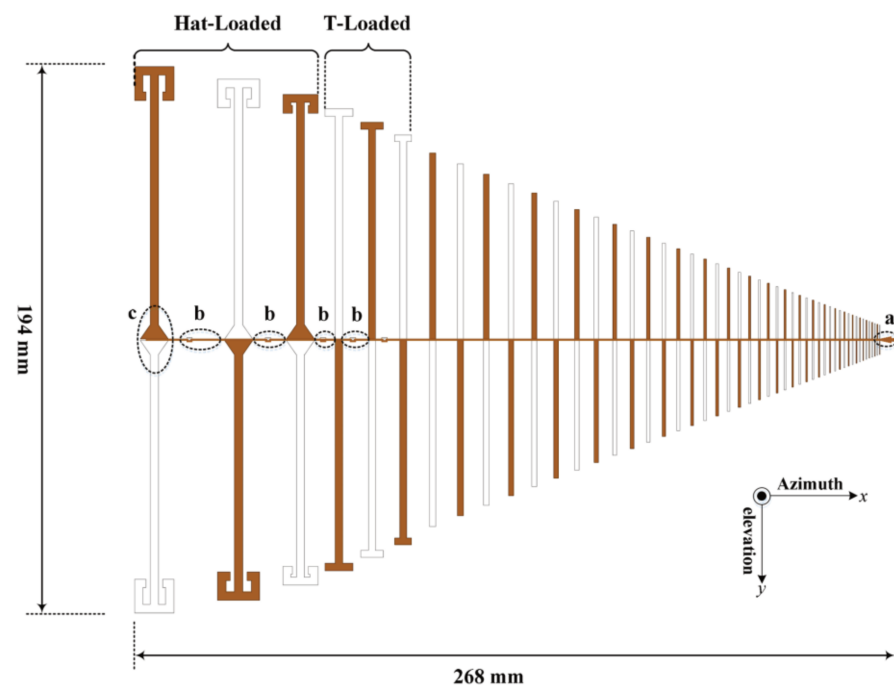


Figure 1. PLPDA design with implemented hat-loading and T-loading techniques in [25].

Another study presents a PLPDA that operates in the frequency range of 8 GHz–18 GHz [26]. In this study, chamfered C-shaped top-loaded elements are introduced to the dipole that acts as an inductive load. This study suggests that the size of a conventional PLPDA can be reduced by 60%. A reduced-size 13-dipole PLPDA with C-shaped loading is designed with an overall size of 33 mm \times 9 mm (length \times width) that can provide a realized gain between 6.1 dBi to 7.1 dBi in the operating frequency range [26]. Figure 2 shows a top view of the CAD model of the PLPDA with the C-shaped loading technique implemented in [26].

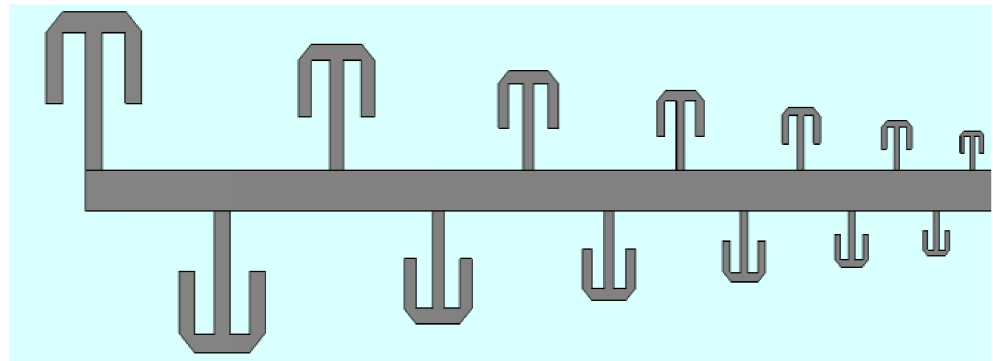


Figure 2. PLPDA design with implemented C-shaped top-loading technique in [26].

A unique variant of T-shaped top loading in the form of circular-arc T-shaped loading is presented in [27]. This study presents an LPDA operating in the frequency range of 0.82–2.09 GHz with an average realized gain of 5 dBi. This study claims a reduction in the dipole lengths by 55%. The reflection coefficient of the antenna depends highly on the radius of the circular arc dipole, and therefore, optimization of the circular arc radius needs to be performed in order to select the correct radius for the required design. Therefore, a similar approach can be used for PLPDA design. Figure 3 shows the implementation of the circular-arc T-shaped loading technique implemented on an LPDA in [27].

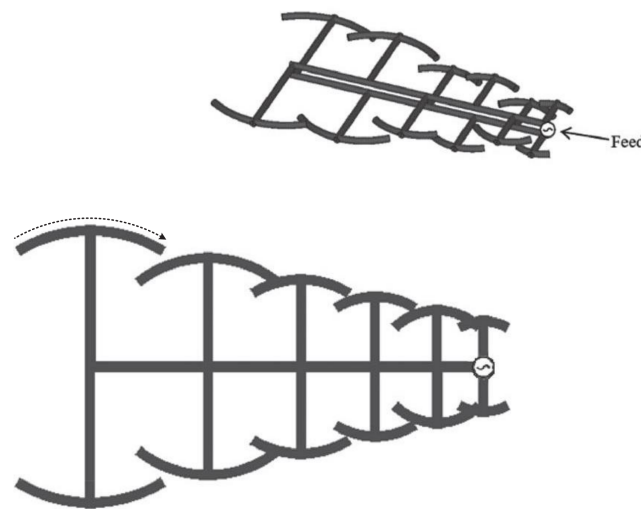


Figure 3. PLPDA design with circular-arc T-shaped loading technique implemented in [27].

An interesting study to reduce the width of PLPDAs is presented in [28], where a PLPDA is designed to operate in the frequency range of 2.3–8 GHz with an average gain of 5–6 dBi. Initially, a nine-dipole conventional PLPDA is designed to operate between 2.3 GHz and 8 GHz. The overall dimension of this conventional PLPDA design is 120 mm × 90 mm (length × width). The size of this conventional PLPDA was reduced by modifying the straight dipoles into T-shaped dipoles in such a way that the total length of the dipole does not change. This method provides a 50% lateral size reduction of the conventional PLPDA, thereby achieving the dimensions of 125 mm × 45 mm. The size of this modified PLPDA was further reduced by introducing double T-shaped dipoles in such a way that the total length remains the same as the straight dipole. By this technique, 54% size reduction was observed in the modified dipole lengths compared to that of the original dipole elements. The overall dimension of this modified PLPDA design with double T-shaped top-loading was found to be 125 mm × 38 mm.

2.2. Fractal-Iterative Technique

An alternate approach to miniaturize a PLPDA, similar to that of top-loading, involves the dipole to consist of fractal shapes in such a way that the total length for the current path is extended. Several fractal shapes can be used as suggested in [29]. Moreover, other fractal shapes such as Minkowski fractal [30], Quasi-Minkowski fractal [31], Koch fractal [32], Triangular Koch fractal [33], square lock fractal [33], tree-fractal [33], peano fractal [33], and meander line [33] are widely used to miniaturize the size of the antenna. A detailed comparison of PLPDAs with different fractal shapes and different iterations is shown in [33] for UWB applications. Additionally, a novel design of PLPDA with Peano fractals at the edge of truncated rhombic branches with spiral slots is also proposed in this reference, that can operate in the UWB band of 3.1–10.6 GHz with a band rejection in the 5.8 GHz and 8.3 GHz band. The proposed PLPDA also provides a gain of more than 5 dBi in the operating frequency range and also leads to miniaturization of the conventional PLPDA by 11.1%. A comparison of several fractal techniques and their miniaturization percentage is shown in Table 1. Figure 4 shows the top view of the CAD model of the PLPDA design with rhombic dipoles terminated using second-order Peano fractals.

Another attempt to miniaturize the conventional PLPDA was demonstrated in [36] using second-order Koch fractals. This reference shows how higher-order Koch fractals can be generated using four iterations. However, the proposed PLPDA antenna in this reference used second-order Koch fractals to miniaturize a nine-dipole conventional PLPDA. The proposed PLPDA has reduced dimensions of 90 mm × 60 mm compared to that of the conventional PLPDA, whose dimensions were 120 mm × 90 mm. This PLPDA operates from 2 GHz to 8 GHz and has an average gain of 5.8 dBi. Figure 5 shows the iterative process used to obtain the second-order Koch fractals in [36].

An interesting approach was suggested in [37], where instead of introducing reactive loading, the concept of a non-uniform transmission line (NTL) was introduced in order to miniaturize the conventional PLPDA. This was completed by the modulation of the impedance profile of straight dipole elements to a truncated Fourier series using optimized Fourier coefficients. This technique achieved a 32% size reduction of the straight dipoles. The proposed PLPDA with truncated Fourier-series dipoles has an operating frequency range of 2–4 GHz and provides a peak gain of 7 dBi. Figure 6 shows the PLPDA design with modified dipoles achieved by optimizing Fourier coefficients [37].

Furthermore, the authors in [38] have presented a compact PLPDA design with meandered line size-reduction technique that covers most of the frequencies in the UWB band. However, the proposed antenna in our paper achieves a wider bandwidth (including the UHF as well as the UWB frequency bands) as well as a higher gain compared to the antenna presented in [38].

Table 1. Comparison of PLPDAs with different fractal shapes.

Reference	Feeding Technique	Fractal Bandwidth	Fractal Shape	Miniaturization
[34]	Microstrip	47%	Koch fractal	12%
[35]	Microstrip	67%	Meander line	21%
[29]	Microstrip	67%	Non-uniform line	32%
[33]	HMSIW	109%	Triangular Koch fractal	11.9%
[33]	HMSIW	109%	Square Koch fractal	10.3%
[33]	HMSIW	109%	Tree fractal—first iteration	27.1%
[33]	HMSIW	109%	Tree fractal—second iteration	35.1%
[33]	HMSIW	109%	Peano fractal in rhombus LPDA	11.1%

HMSIW = half-mode surface integrated waveguide.

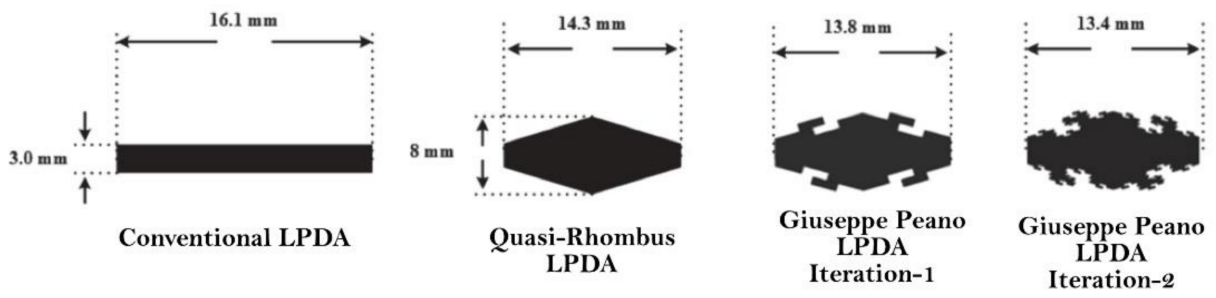


Figure 4. PLPDA design with rhombic dipoles terminated using Peano fractals in [33].

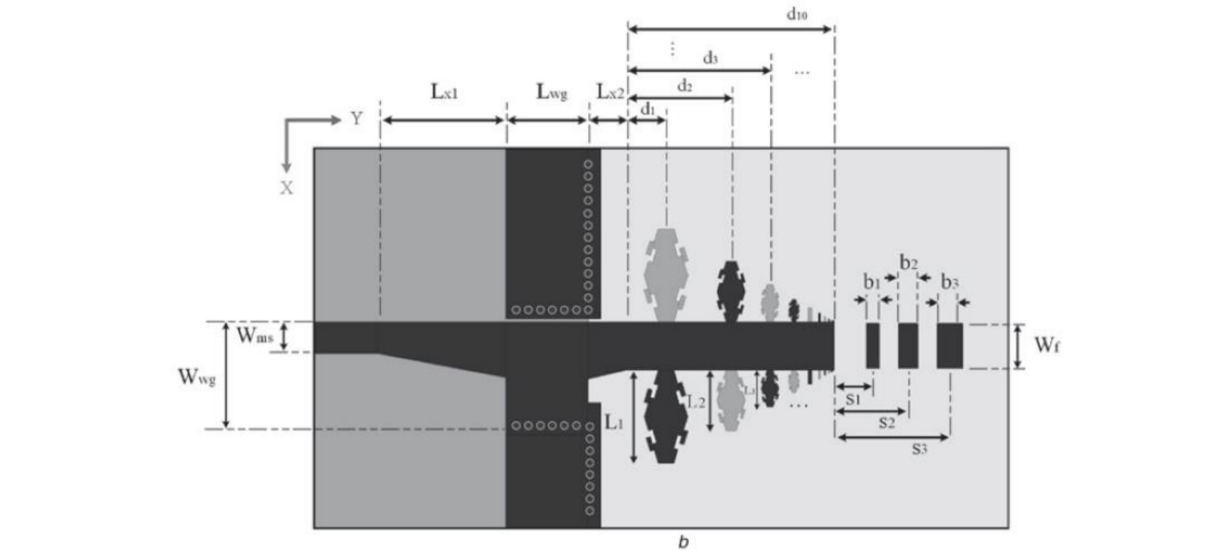


Figure 5. Shape of second-order Koch fractals used as dipoles in PLPDA design in [36].

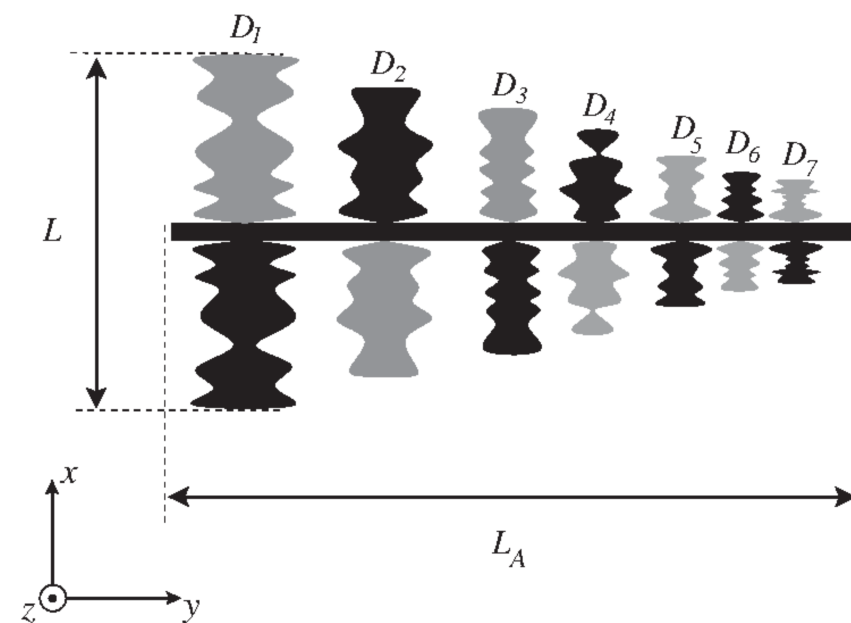
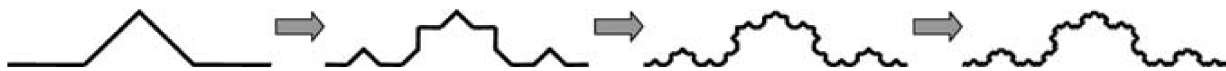


Figure 6. PLPDA design with modified dipoles using optimized Fourier coefficients [37].

2.3. Truncated Boom Technique

Most of the miniaturization techniques are applied to the longest dipole of the PLPDA in order to reduce the lateral size of the PLPDA. For instance, the Koch Fractalization method in [30,35,39], top-loading in [25,27,28,40], and metamaterials in [40,41] are mostly applied to the longer dipoles so that the lateral size of the PLPDA is reduced. However, a unique and useful approach is proposed in [42] that can be used to reduce the axial size of the PLPDA by reducing the boom length. The authors in [42] propose the use of dual-band dipoles instead of single-band straight dipoles. In this way, the number of dipoles required by the PLPDA to cover a wide operating band reduces, which in turn also reduces the boom length. The dual-band dipole is designed in such a way that it has a half-wave principle dipole which is then loaded with an auxiliary dipole that acts as a resistive load. This dual-band dipole then follows the conventional PLPDA pattern. The PLPDA proposed in [42] consists of 25 dual-band dipoles, and the antenna operates from 0.5 GHz to 10 GHz. The proposed design results in a 40% size reduction in the total axial length of the PLPDA compared to that of the conventional PLPDA. Additionally, the number of dipoles required to achieve the same performance as 66 dipoles is reduced to just 25 dipoles in the proposed PLPDA design. The total axial length in the case of the 66-dipole conventional PLPDA was 364 mm, and it was reduced to 218 mm in the case of the proposed 25 dual-band dipole PLPDA. Additionally, it was also observed that if a conventional PLPDA of the same length as that of the proposed PLPDA was designed with a reduced spacing factor, the total bandwidth was 58% lower compared to the proposed PLPDA. The overall dimensions of the proposed PLPDA are 218 mm \times 260 mm (axial length \times lateral length). The proposed PLPDA uses a Rogers RO4003 substrate with a dielectric constant of 3.55 and substrate thickness of 0.508 mm. The antenna is claimed to achieve a 5 dBi gain in the entire bandwidth. The only limitation to this technique is that the gain of the antenna is reduced. However, several gain enhancement techniques can be used to increase the gain of the proposed PLPDA antenna. Figure 7 shows the top view of the CAD model of PLPDA design with dual-band dipoles from [42].

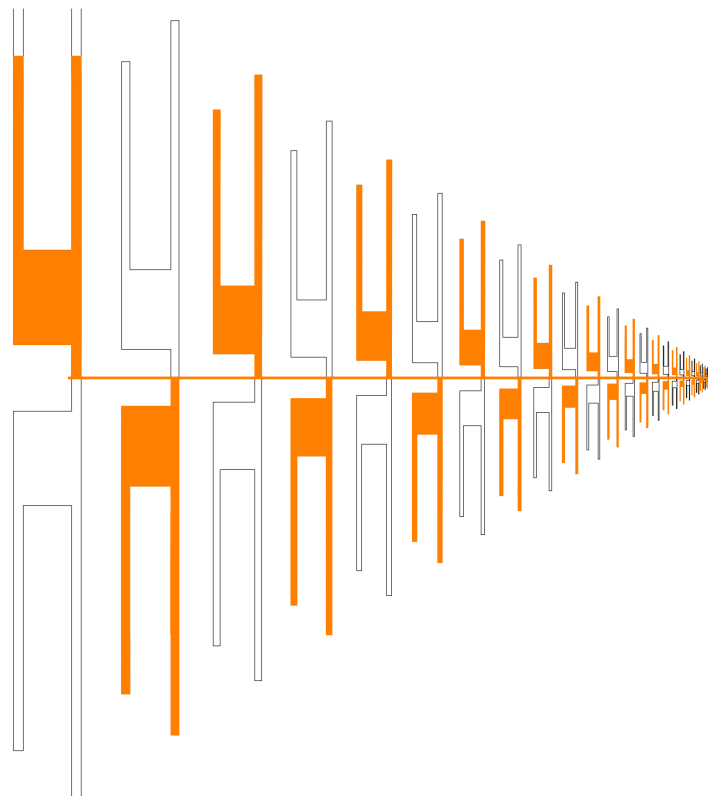


Figure 7. PLPDA design with dual-band dipoles [42].

2.4. Reflector Ground Plane Technique for Gain Enhancement

Several miniaturization techniques result in reduced size of the antenna; however, in several cases, the gain of the antenna drops after miniaturization. An interesting approach is presented in [43], where a PLPDA is proposed that has an operating frequency range of 3.3–20.7 GHz with an average gain of 6 dBi. The PLPDA design consists of 17 dipoles that follow the conventional PLPDA design. In addition to this, a ground plane is added after the longest dipole on both sides of the substrate as proposed in [43]. This ground plane acts as a reflector and thus provides increased gain for the antenna. The antenna was fabricated on an FR-4 substrate with dielectric constant of 4.4 and substrate thickness of 1.6 mm. In addition to this, the authors also demonstrate an interesting approach to provide band rejection in the operating bandwidth using U-shaped notches. A U-shaped slot is placed on the boom of the antenna and its position is optimized until the required band rejection is obtained. The design proposed in this paper makes use of a U-shaped slot that has dimensions of 6.87 mm × 2.6 mm (length × width) in order to achieve a rejection in the 5.8 GHz WLAN band.

A similar approach to increase the gain of an PLPDA is proposed in [44], where a substrate integrated waveguide (SIW) is used after the longest dipole. The SIW acts as a reflector that leads to an increase in gain. Furthermore, the gain of the PLPDA was further increased by adding parasitic patches after the end of the shortest dipole, which act as directors. This approach involves the idea of combining the benefits of log-periodic antennas and quasi-Yagi antennas. The proposed antenna is designed to operate from 40 GHz to 50 GHz and in addition to this, it is also claimed to achieve a gain between 9 and 12.6 dBi. The technique of combining quasi-Yagi and log-periodic designs provides a gain enhancement of around 2.5 dB to 3.4 dB compared to the conventional PLPDA [44].

2.5. Dielectric Loading Technique

A novel and useful technique to miniaturize the conventional PLPDA using two-stepped dielectric materials by adopting the dielectric-loading technique is presented in [45]. The PLPDA proposed in this reference operates in the frequency range of 200–803 MHz and provides a gain greater than 4 dBi. The design proposed in this study suggests utilizing 22-sinusoidal dipoles instead of straight dipoles, as shown in Figure 8. The reason to use sinusoidal dipoles is that they provide extended current paths and can also provide resonance at lower frequencies as compared to straight dipoles. A Polyflon substrate of a dielectric constant of 2.55 and loss tangent of 0.0011 is used to fabricate the antenna. The thickness of this substrate is 3 mm. The uniqueness of this design is that it includes a 2 mm thick layer of air that is partially loaded within this substrate. The additional size reduction of the antenna is obtained by using a two-stepped dielectric material of dielectric constant of 10 and loss tangent of 0.0035 that is used to cover the antenna from both sides. Furthermore, four parasitic elements are added at the end of the first two sinusoidal dipoles in order to implement the capacitive loading technique to reduce the size of the antenna. The overall size of this antenna is 576.6 mm × 420 mm × 29.6 mm (length × width × thickness). Since this antenna has a high power-handling capacity, it can find applications in airborne platforms.

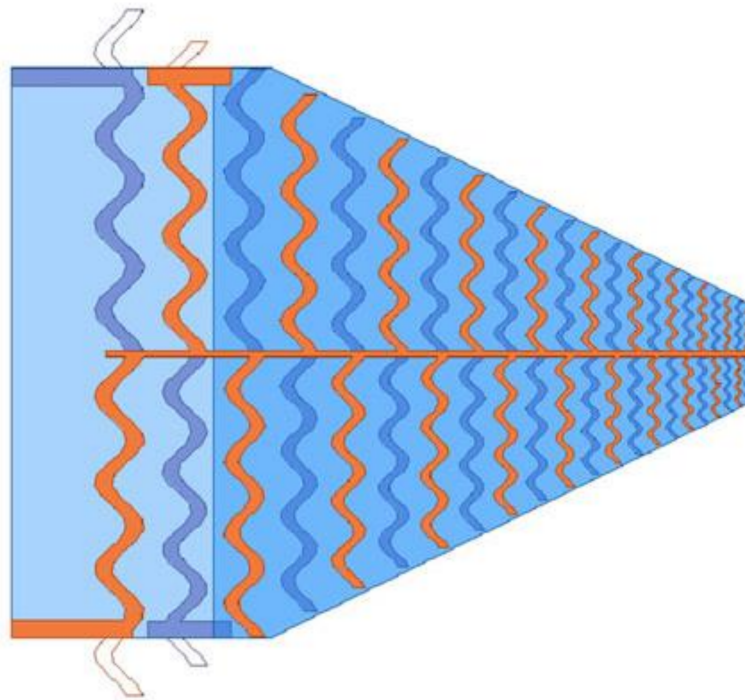


Figure 8. PLPDA design with dielectric-loading technique [45].

2.6. *Folded-Planar Helix (FPH) Dipole*

There have been successful attempts to miniaturize the PLPDA by replacing the straight dipoles with different sized and/or shaped dipoles to reduce the lateral size of the antenna. However, most of these techniques lead to a deterioration of gain. A similar, yet useful, approach is proposed in [46], where the straight dipoles are replaced with folded planar helix (FPH) dipoles, as shown in Figure 9. Implementing this technique leads to a reduction of the dipole size by 39%. In addition to that, it leads to a deterioration of gain by only 0.2 dB, which is much smaller compared to other miniaturization techniques. The proposed PLPDA had an operating frequency range of 400–800 MHz. An initial design was achieved by replacing the longest straight dipole with an FPH dipole, which led to a size reduction of 18.2%. However, when two FPH dipoles were used, the size was further reduced, and a total reduction of 39% was obtained compared to the conventional PLPDA. This technique also gives an improvement in the front-to-back ratio of the antenna and achieves a gain of 5.5 dBi. Both the proposed antennas are designed on an FR4 substrate with a dielectric constant of 4.4 and substrate thickness of 3.2 mm. The overall dimensions of the proposed PLPDA using a meander dipole between the 2 FPH dipole elements is 445 mm × 273 mm × 3.2 mm.

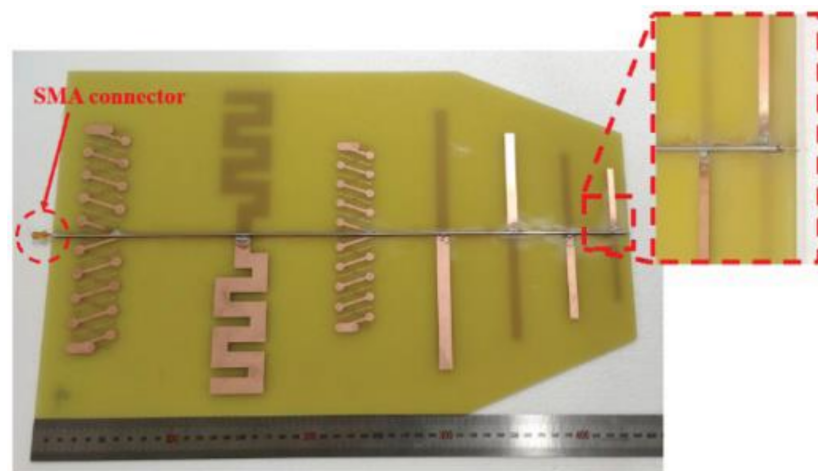


Figure 9. PLPDA design with two folded-planar helix dipoles [46].

3. Conventional PLPDA Design for 0.7 GHz–8 GHz

This section presents a wideband 25-dipole PLPDA that has an operating range from 0.7 GHz to 8 GHz. The antenna dimensions for the PLPDA were derived using traditional LPDA equations introduced by Carrel [19,20] and then calculating the dimensions with the effect of relative permittivity of the antenna substrate. A schematic diagram of the conventional LPDA antenna is shown in Figure 10.

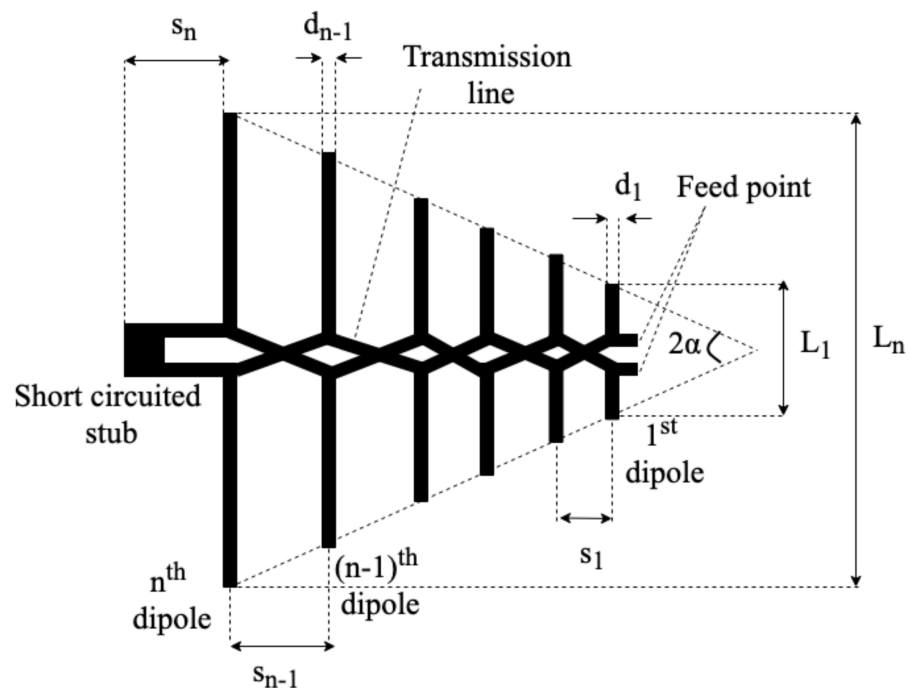


Figure 10. Schematic diagram of the conventional LPDA.

The apex angle is the half-angle in which all the dipoles are confined, and it is mathematically expressed as

$$\alpha = \tan^{-1} \left[\frac{1 - \tau}{4\sigma} \right] \quad (1)$$

In the above expression, the parameter τ is called the “scaling factor”, and is the ratio of the lengths or diameters of two consecutive dipoles as shown by the following expression:

$$\tau = \frac{L_{n+1}}{L_n} = \frac{d_{n+1}}{d_n} \quad (2)$$

where L_n and d_n are, respectively, the length and the diameter of the n th dipole. Additionally, the parameter σ shown in (1) is called the “spacing factor” and is defined as:

$$\sigma = \frac{s_n}{2L_n} \quad (3)$$

where s_n is the spacing between the n th dipole and its consecutive $(n + 1)$ th dipole. The overall physical dimensions of the antenna significantly depend on the above two factors (τ and σ).

The antenna design was required to provide a gain of above 5 dBi in its entire operating range, and thus, in order to satisfy the bandwidth and gain specifications, 25 dipoles were selected. Similar to traditional LPDAs, this PLPDA also consists of dipoles that are arranged in an increasing fashion from the front to the back part of the antenna. The only difference is the dielectric substrate (FR4), with a relative permittivity of 4.3, is present between the top and the bottom boom instead of air. Therefore, it can be suggested that the top boom and the dipoles attached to it are embedded on the top part of the substrate, while the bottom boom and the dipoles attached to it are attached to the bottom part of the substrate. The thickness of the substrate is 1 mm. The feeding is provided to the antenna using a coaxial cable that is connected to the top boom using solder paste. The conducting part of the cable is soldered to the start of the bottom boom through a drilled hole. The overall dimensions of the proposed antenna are: 250 mm \times 170 mm \times 1 mm (length \times width \times thickness). The simulated and the fabricated model of the antenna is shown in Figure 11.

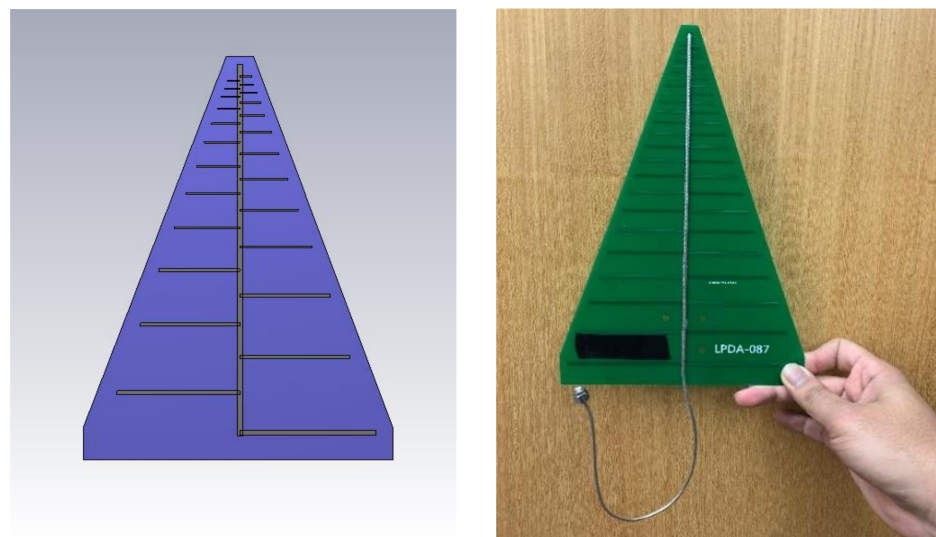


Figure 11. CST model (left) and fabricated model (right) of the conventional PLPDA antenna.

The CST model consisted of 83,184,192 hexahedral mesh cells with the smallest cell size of 0.35 mm. The simulation of this model was performed in the time domain with -50 dB accuracy and hardware acceleration using an Nvidia GP100 GPU. The dimensions of this antenna are listed in Table 2. Where

- L_n = length of n^{th} dipole;
- s_n = spacing between n^{th} and $(n+1)^{\text{th}}$ dipole;
- d_n = width of n^{th} dipole;
- L-boom = length of the boom;
- W-boom = width of the boom;
- H-boom = thickness of the boom (equivalent to copper clad thickness in this case).

Table 2. Dimensions of the conventional PLPDA antenna.

Parameters	Values	Parameters	Values	Parameter	Values
L1	5 mm	L14	22 mm	d1	0.5
L2	5.5 mm	L15	25 mm	d2	0.5
L3	6 mm	L16	28 mm	d3	0.5
L4	7 mm	L17	30.5 mm	d4	0.5
L5	8 mm	L18	34.5 mm	d5	0.5
L6	9 mm	L19	38 mm	d6	0.6
L7	10 mm	L20	43 mm	d7	0.7
L8	11 mm	L21	48 mm	d8	0.8
L9	12 mm	L22	53 mm	d9	0.9
L10	14 mm	L23	59 mm	d10	1 mm
L11	16 mm	L24	66 mm	d11	1 mm
L12	18 mm	L25	73 mm	d12	1 mm
L13	20 mm	s13	7 mm	d13	1 mm
s0	7 mm	s14	7 mm	d14	1 mm
s1	2 mm	s15	8 mm	d15	1 mm
s2	2 mm	s16	9 mm	d16	1 mm
s3	2 mm	s17	10 mm	d17	1 mm
s4	2 mm	s18	11 mm	d18	1 mm
s5	2 mm	s19	13 mm	d19	1 mm
s6	3 mm	s20	14 mm	d20	1.5 mm
s7	3 mm	s21	16 mm	d21	2 mm
s8	3.5 mm	s22	18 mm	d22	2 mm
s9	4 mm	s23	20 mm	d23	2 mm
s10	4.5 mm	s24	22 mm	d24	2.5 mm
s11	5 mm	L-boom	230 mm	d25	3 mm
s12	6 mm	H-boom	35 μm	W-boom	3 mm

The fabricated antenna was measured in an outdoor far-field measurement facility at the University of Huddersfield using a portable FSH8 Rohde & Schwarz vector network analyzer. The gain measurements were performed using the two-antenna method, where two identical fabricated antennas were used to measure the S12 coefficient from one antenna to the other.

Figure 12 presents a comparison of the simulated and the measured return loss of the proposed antenna design. The graph suggests that the antenna has a low S11 below -10 dB in its entire operating frequency range from 0.7 GHz to 8 GHz. Thus, the antenna achieves good matching. Moreover, the graph also suggests that the simulated results are generally in good agreement with the measurements.

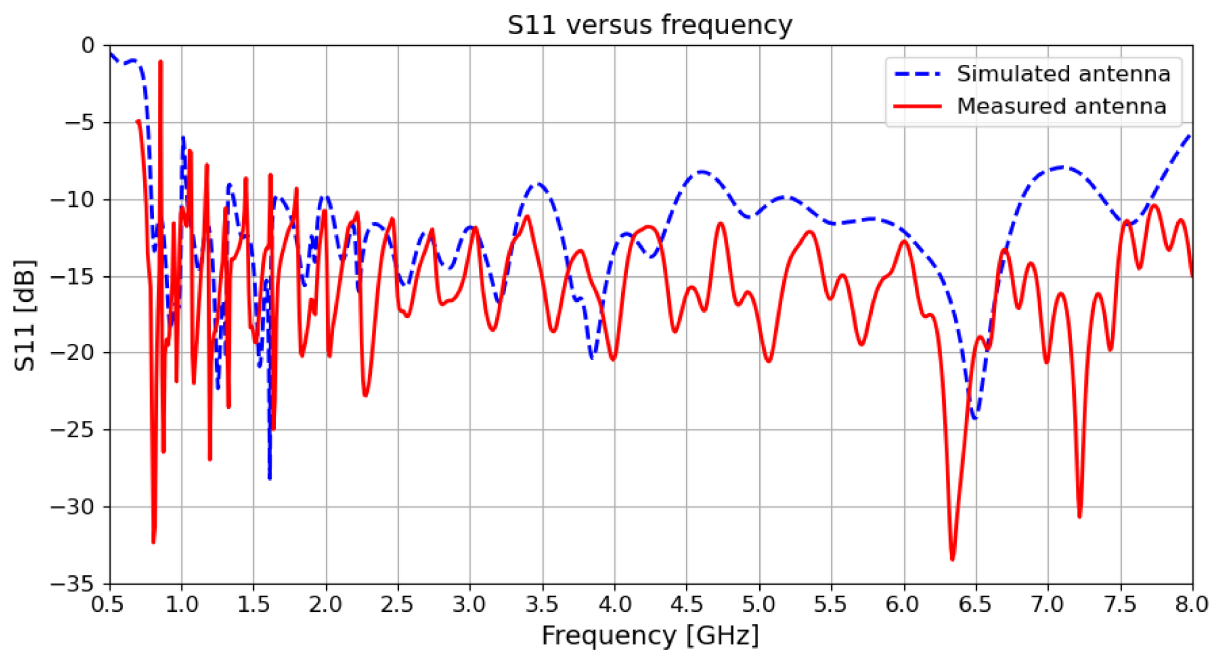


Figure 12. Comparison of the simulated and measured S11 of the conventional PLPDA design.

Figure 13 shows a comparison of the simulated and the measured realized gain of the antenna. The antenna achieves a flat gain of approximately 5.5 dBi in its operating frequency range. The measured and simulated results are in good agreement. The gain of the antenna was measured using the two-antenna method.

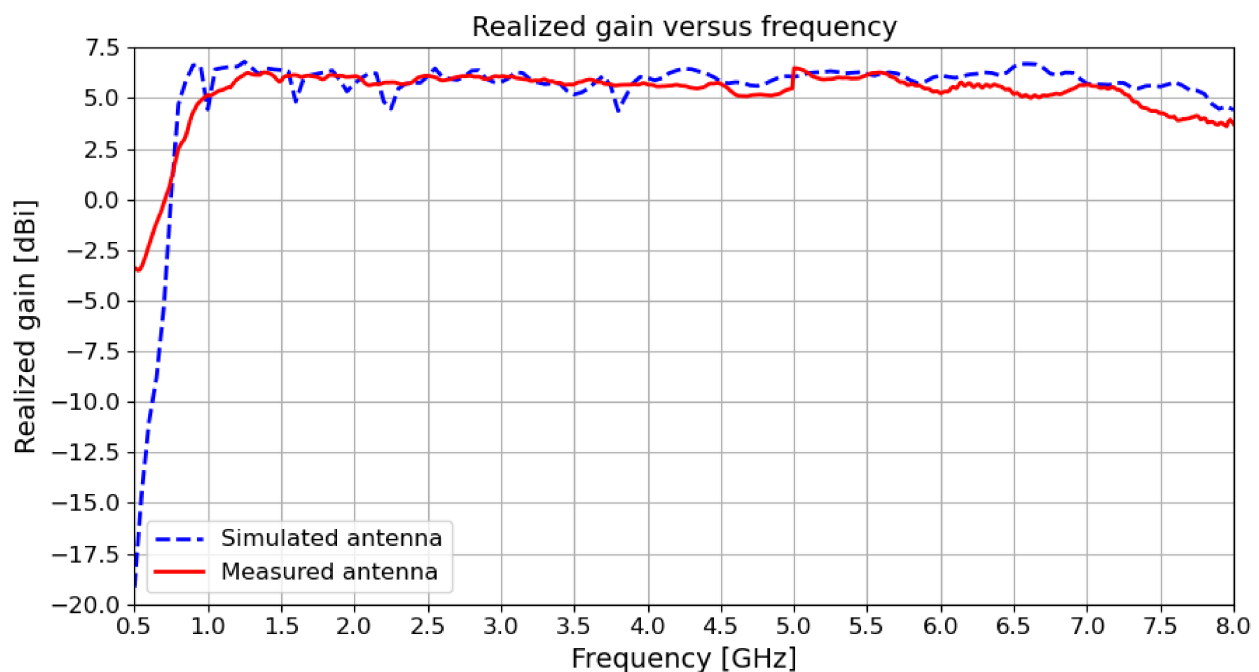


Figure 13. Comparison of the simulated and the fabricated realized gain of the conventional PLPDA antenna.

4. Extended Low-Frequency Response PLPDA Design for 0.4 GHz–8 GHz

In order to extend the lowest operating frequency of the antenna proposed in Section 3, a novel antenna is proposed in this section that operates in the frequency range from 0.4 GHz to 8 GHz. From the principle of operation of traditional PLPDAs, it is clear that the performance of the antenna at lower frequencies depends on the longest few

dipoles. Therefore, the longest straight dipole was replaced by a triangular dipole in order to increase the gain and bandwidth of the antenna. With the introduction of this new dipole type, an optimization of the longest four dipole lengths, three spacings, and four dipole widths was performed using Trust Region Framework (TRF) algorithm in CST. However, several other optimization algorithms could also have been used, such as Particle Swarm Optimization (PSO) in [47,48], PSOvm (PSO velocity mutation) in [49,50], and Invasive Weed Optimization (IWO) in [51–54]. Furthermore, a comparative study of several optimization algorithms is presented in [55]. The optimization goals were set to obtain S11 below -12 dB and a higher gain above 5.5 dB between 0.4 GHz and 1.2 GHz. The remaining dipoles and frequencies that were not considered as the optimization would not significantly affect the frequencies higher than 1.2 GHz, as only the four longest dipole dimensions were considered. The optimization goals can be clearly visualized in Table 3.

Table 3. Optimization goals.

Parameters	Goals	Frequency (MHz)	Weight
S11	< -12 dB	0.4 GHz–1.2 GHz.	5.0
Realized gain	> 5 dBi	0.4 GHz–1.2 GHz	5.0

Figure 14 shows the CST model of the optimized antenna. The model consisted of 92,452,080 hexahedral mesh cells with the smallest cell unit of 0.35 mm. The simulations were performed in the time-domain with a -50 dB accuracy and hardware acceleration with an Nvidia GP100 GPU. The overall dimensions of the optimized PLPDA are 270 mm \times 279 mm \times 1 mm (length \times width \times thickness). If the same antenna were designed using the conventional PLPDA design equations, the overall dimensions of this antenna would be approximately 380 mm \times 300 mm \times 1 mm. Thus, it is evident that the improved PLPDA is 29% reduced in terms of length compared to a conventional PLPDA designed for the same frequency range.

Furthermore, the dimensions of the improved PLPDA antenna are shown in Table 4.

Figure 15 presents the simulated S11 of the proposed PLPDA. It suggests that the antenna has good matching with low S11 values below -10 dB in most of the operating frequency range. Further improvement is required at some frequencies.

Figure 16 shows the simulated realized gain of the proposed antenna. The graph suggests that the antenna provides a gain of above 5.5 dBi in most of its frequency range; however, lower values of gain are observed from 0.4 GHz to 1 GHz. However, realized gain is significantly higher in the lower frequencies than that of the conventional design with an antenna that is only marginally longer (270 mm instead of 250 mm) but significantly wider (279 mm instead of 170 mm). The performance of the proposed antenna can be further improved by introducing other gain enhancement techniques and re-optimizing the antenna.

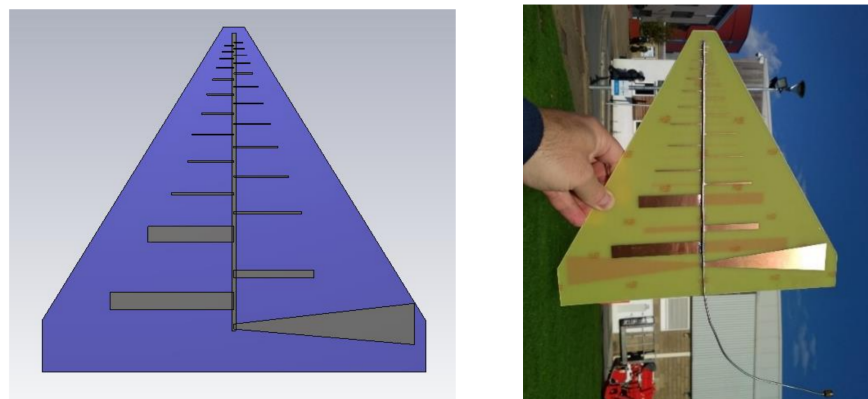


Figure 14. CST model of the proposed PLPDA.

Table 4. Dimensions of the improved PLPDA antenna.

Parameters	Values	Parameters	Values	Parameter	Values
L1	5 mm	L14	22 mm	d1	0.5
L2	5.5 mm	L15	25 mm	d2	0.5
L3	6 mm	L16	28 mm	d3	0.5
L4	7 mm	L17	30.5 mm	d4	0.5
L5	8 mm	L18	34.5 mm	d5	0.5
L6	9 mm	L19	38 mm	d6	0.6
L7	10 mm	L20	43 mm	d7	0.7
L8	11 mm	L21	48 mm	d8	0.8
L9	12 mm	L22	60.9 mm	d9	0.9
L10	14 mm	L23	56.5 mm	d10	1 mm
L11	16 mm	L24	88.3 mm	d11	1 mm
L12	18 mm	L25	130 mm	d12	1 mm
L13	20 mm	s13	7 mm	d13	1 mm
s0	7 mm	s14	7 mm	d14	1 mm
s1	2 mm	s15	8 mm	d15	1 mm
s2	2 mm	s16	9 mm	d16	1 mm
s3	2 mm	s17	10 mm	d17	1 mm
s4	2 mm	s18	11 mm	d18	1 mm
s5	2 mm	s19	13 mm	d19	1 mm
s6	3 mm	s20	14 mm	d20	1.5 mm
s7	3 mm	s21	9.5 mm	d21	2 mm
s8	3.5 mm	s22	21.5 mm	d22	12.4 mm
s9	4 mm	s23	11 mm	d23	6.4 mm
s10	4.5 mm	s24	11 mm	d24	13.8 mm
s11	5 mm	L-boom	230 mm	d25	32.3 mm
s12	6 mm	H-boom	35 μ m	W-boom	3 mm

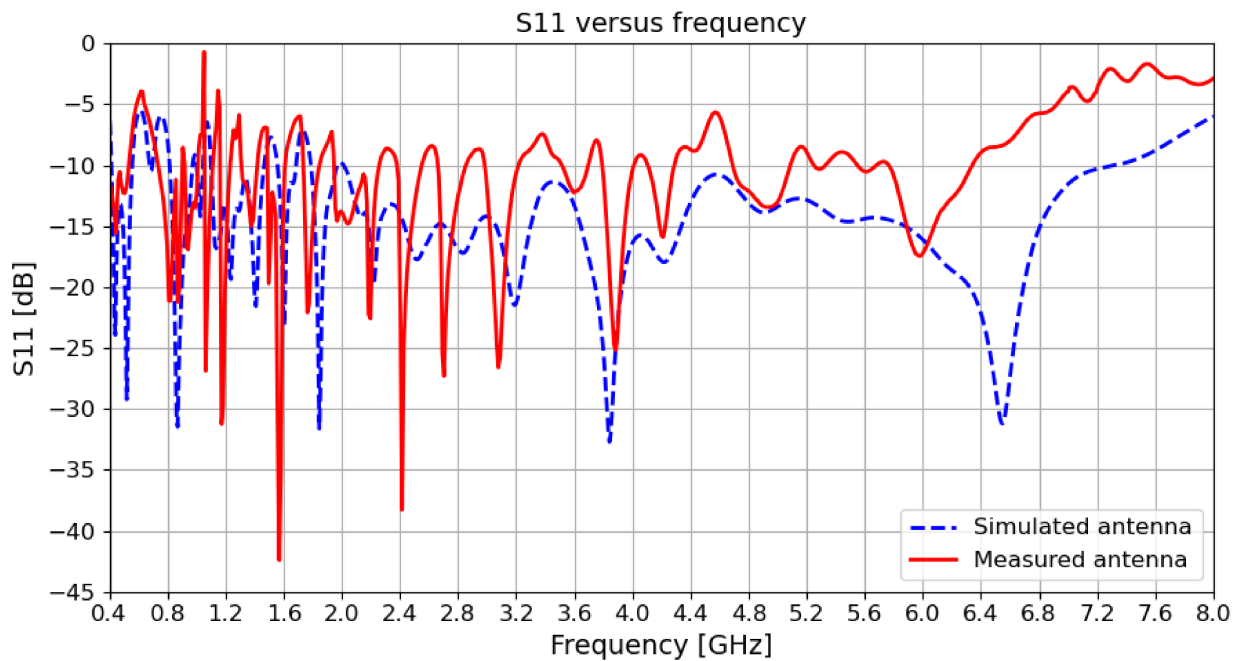


Figure 15. S11 of the improved PLPDA design.

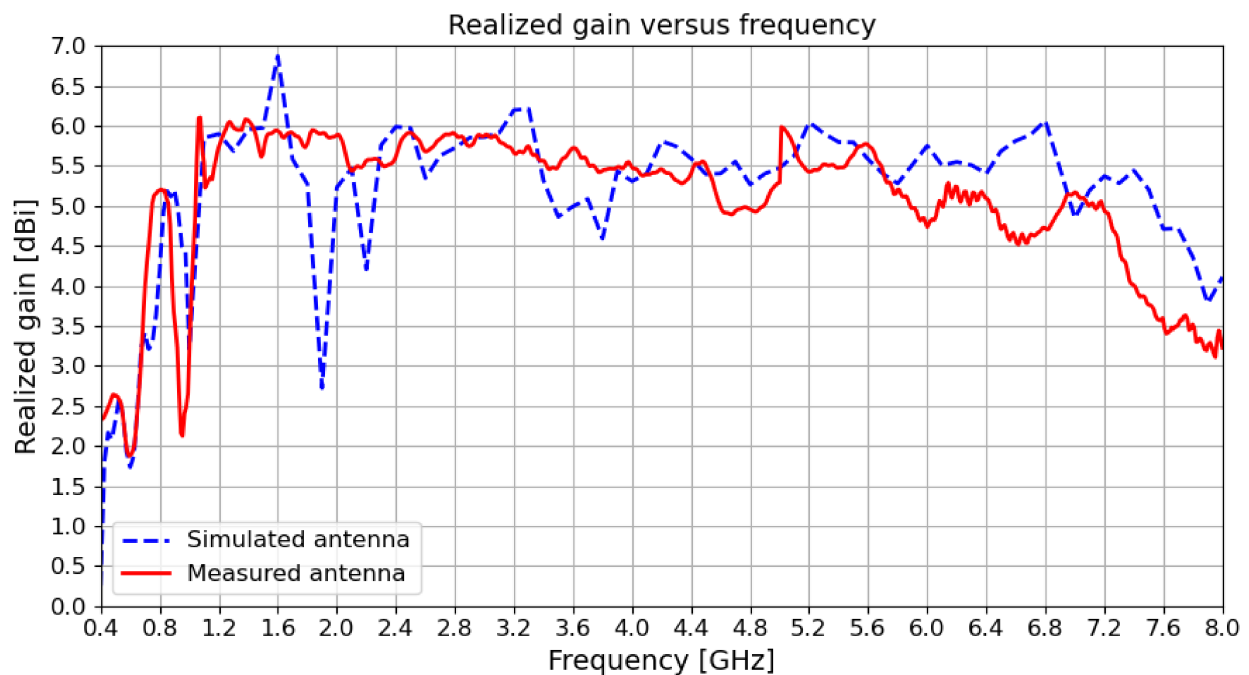


Figure 16. Realized gain of the improved PLPDA design.

Figure 17 shows the front-to-back ratio of the proposed PLPDA design. It shows that the antenna presents highly directional characteristics; however, further improvements can be made to the antenna performance from 0.4 GHz to 0.7 GHz.

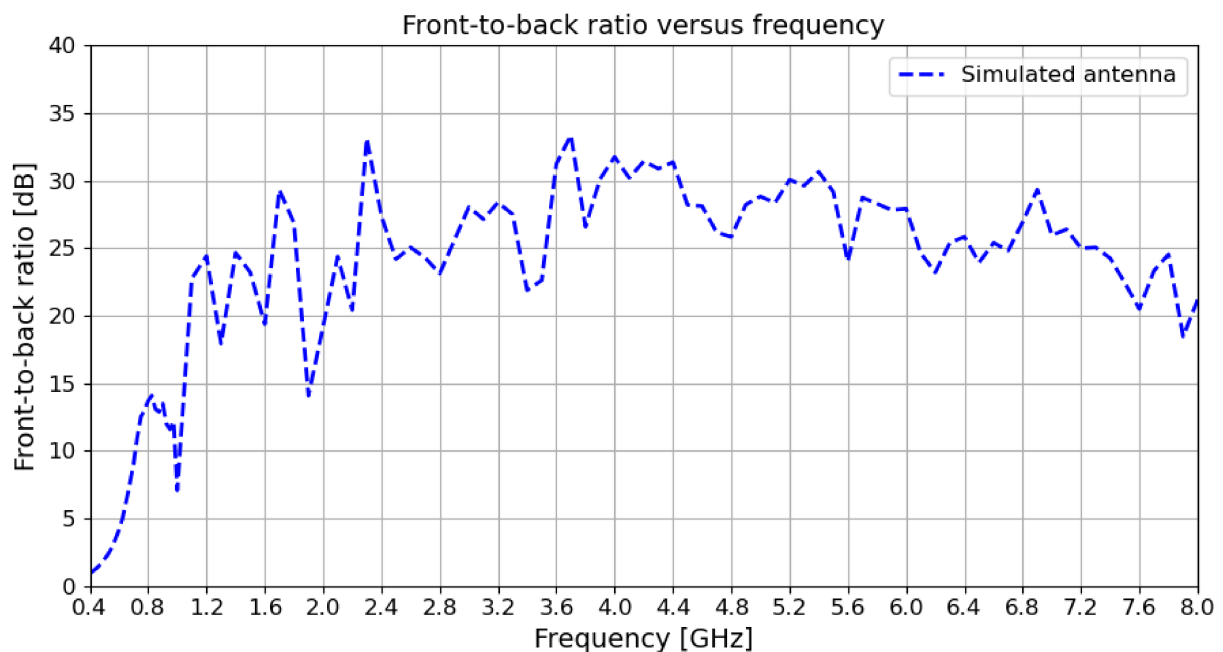


Figure 17. Front-to-back ratio of the improved PLPDA design.

Figure 18 shows the polar plots of the simulated E-plane radiation pattern of the improved PLPDA design at (a) 0.4 GHz, (b) 0.8 GHz, (c) 2 GHz, (d) 4 GHz, (e) 6 GHz, and (f) 8 GHz, respectively. It also suggests that the antenna demonstrates stable radiation patterns across the frequency bandwidth.

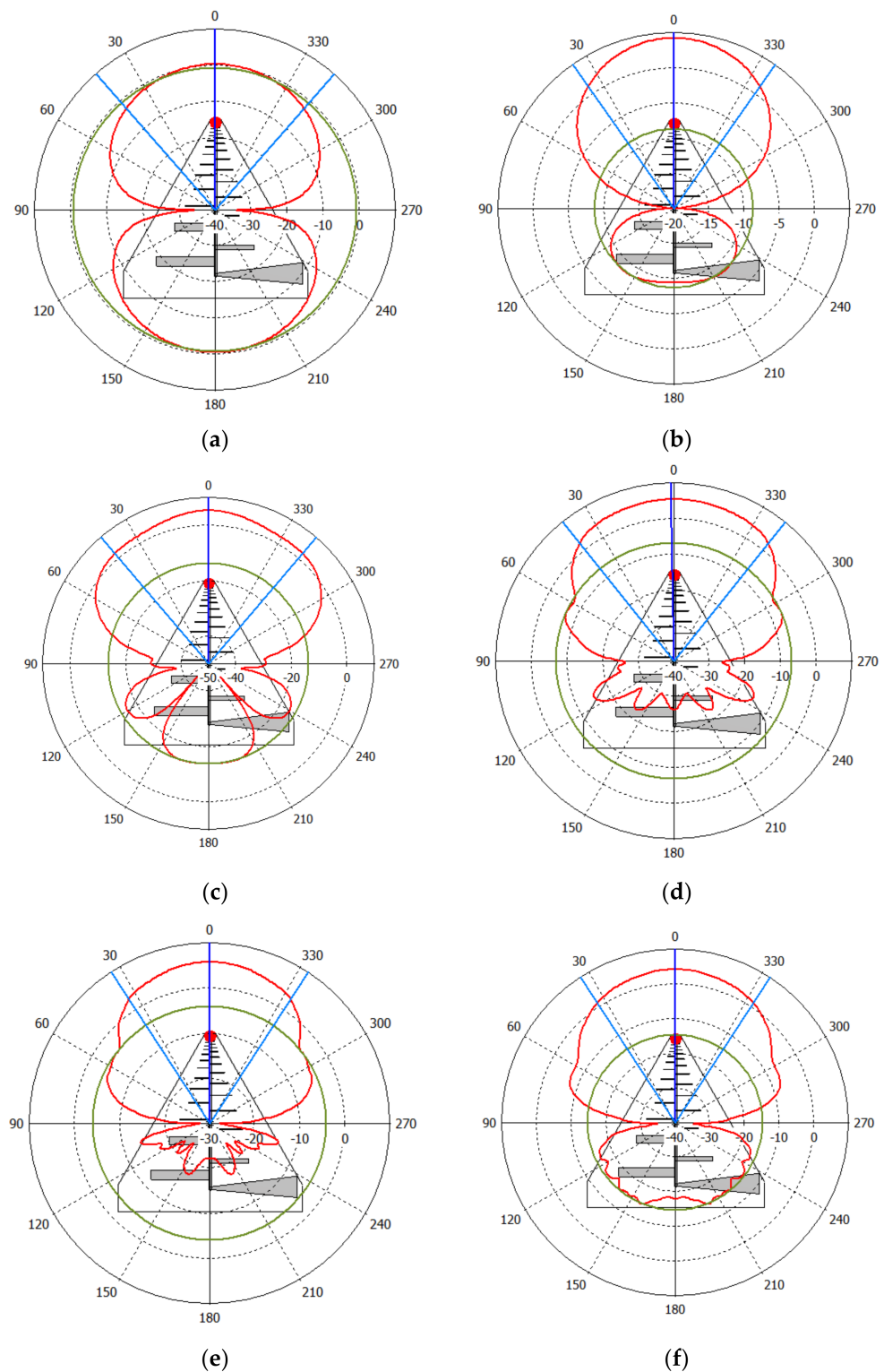


Figure 18. Polar plots of the E-plane radiation patterns of the proposed antenna at (a) 0.4 GHz, (b) 0.8 GHz, (c) 2 GHz, (d) 4 GHz, (e) 6 GHz, and (f) 8 GHz.

5. Conclusions

This paper reviews several miniaturization techniques to reduce the size of PLPDAs. Two prototypes of PLPDAs are proposed that operate in a wide bandwidth. The first prototype proposed is a 25-dipole PLPDA that operates from 0.7 GHz to 8 GHz and provides a gain of above 5.5 dBi. The second prototype is an optimized design of the first prototype that includes a triangular longest dipole instead of the straight dipole. Replacing

the shape of the longest dipole and optimizing the lengths, diameters, and spacings of the longest four dipoles provides a higher bandwidth compared to the first prototype. The optimized design operates from 0.4 GHz to 8 GHz and provides a gain of above 5 dBi in most of its bandwidth. The TRF algorithm was used in the optimization.

Author Contributions: Conceptualization, K.K.M. and P.I.L.; methodology, K.K.M., P.I.L. and Z.D.Z.; software, K.K.M.; validation, P.I.L. and Z.D.Z.; formal analysis, K.K.M. and P.I.L.; investigation, K.K.M. and P.I.L.; resources, P.I.L. and T.H.L.; data curation, K.K.M. and T.H.L.; writing—original draft preparation, K.K.M. and P.I.L.; writing—review and editing, Z.D.Z.; visualization, K.K.M.; supervision, P.I.L. and Z.D.Z.; project administration, P.I.L.; funding acquisition, P.I.L. All authors have read and agreed to the published version of the manuscript.

Funding: This research was partially funded by the “European Union’s Horizon 2020 research and innovation programme under the Marie Skłodowska-Curie”, grant agreement number 861219, and the “European Union’s Horizon 2020 Research and Innovation Staff Exchange programme”, grant agreement number 872857.

Acknowledgments: The work of T. H. Loh was supported by the 2021–2025 National Measurement System Programme of the U.K. Government’s Department for Business, Energy and Industrial Strategy, through the Science Theme Reference EMT21 of that Programme.

Conflicts of Interest: The authors declare no conflict of interest.

References

1. FCC. FCC First Report and Order on Ultra-Wideband Technology. Available online: https://transition.fcc.gov/Bureaus/Engineering_Technology/Orders/2002/fcc02048.pdf (accessed on 25 June 2021).
2. ECC Std. ECC Decision of 24 March 2006 on the Harmonised Conditions for Devices Using Ultra-Wideband (UWB) Technology in Bands Below 10.6 GHz. 2006. Available online: <http://www.ero.dk/> (accessed on 25 June 2021).
3. Liang, J.; Chiau, C.C.; Chen, X.; Parini, C.G. Study of a printed circular disc monopole antenna for UWB systems. *IEEE Trans. Antennas Propag.* **2005**, *53*, 3500–3504. [[CrossRef](#)]
4. Mohamadzade, B.; Simorangkir, R.B.V.B.; Hashmi, R.M.; Lalbakhsh, A. A Conformal Ultrawideband Antenna with Monopole-Like Radiation Patterns. *IEEE Trans. Antennas Propag.* **2020**, *68*, 6383–6388. [[CrossRef](#)]
5. Das, P.; Mandal, K.; Lalbakhsh, A. Single-layer polarization-insensitive frequency selective surface for beam reconfigurability of monopole antennas. *J. Electromagn. Waves Appl.* **2019**, *34*, 86–102. [[CrossRef](#)]
6. Azim, R.; Islam, M.T.; Misran, N. Compact Tapered-Shape Slot Antenna for UWB Applications. *IEEE Antennas Wirel. Propag. Lett.* **2011**, *10*, 1190–1193. [[CrossRef](#)]
7. Tsai, C.-L.; Yang, C.-L. Novel Compact Eye-Shaped UWB Antennas. *IEEE Antennas Wirel. Propag. Lett.* **2012**, *11*, 184–187. [[CrossRef](#)]
8. Gautam, A.K.; Yadav, S.; Kanaujia, B. A CPW-Fed Compact UWB Microstrip Antenna. *IEEE Antennas Wirel. Propag. Lett.* **2013**, *12*, 151–154. [[CrossRef](#)]
9. Mistry, K.K.; Lazaridis, P.I.; Zaharis, Z.D.; Chochliouros, I.P.; Loh, T.H.; Gravas, I.P.; Cheadle, D. Optimization of Log-Periodic TV Reception Antenna with UHF Mobile Communications Band Rejection. *Electronics* **2020**, *9*, 1830. [[CrossRef](#)]
10. Mistry, K.; Lazaridis, P.; Zaharis, Z.; Xenos, T.; Glover, I. Optimization of log-periodic dipole antenna with LTE band-rejection. In Proceedings of the Loughborough Antennas & Propagation Conference (LAPC 2017), Loughborough, UK, 13–14 November 2017; Institution of Engineering and Technology (IET): Stevenage, UK, 2017; p. 84.
11. Lazaridis, P. Log-Periodic Antenna with a Passband and a Stopband. US Patent GB2568280A, 15 May 2019.
12. Yeo, J.; Lee, J.I. Miniaturized LPDA antenna for portable direction-finding applications. *ETRI J.* **2012**, *34*, 118–121. [[CrossRef](#)]
13. Harrison, R.W.; Jessup, M. A novel log periodic implementation of a 700 MHz–6 GHz slant polarised fixed-beam antenna array for direction finding applications. In Proceedings of the 2012 42nd European Microwave Conference, Amsterdam, The Netherlands, 29 October–1 November 2012; pp. 727–730.
14. Liang, X.; Chia, Y.; Chia, M.Y.W. New precision wideband direction finding antenna. *IEE Proc. Microw. Antennas Propag.* **2001**, *148*, 363. [[CrossRef](#)]
15. Huang, Y.; Boyle, K. *Antennas: From Theory to Practice*; John Wiley & Sons: Hoboken, NJ, USA, 2008.
16. Isbell, D. Log periodic dipole arrays. *IRE Trans. Antennas Propag.* **1960**, *8*, 260–267. [[CrossRef](#)]
17. Rumsey, V. Frequency independent antennas. In Proceedings of the 1958 IRE International Convention Record, New York, NY, USA, 21–25 March 1966; Volume 5, pp. 114–118.
18. Duhamel, R.; Ore, F. Logarithmically periodic antenna designs. *IRE Int. Conv. Rec.* **2005**, *6*, 139–151. [[CrossRef](#)]
19. Carrel, R.L. *Analysis and Design of the Log-Periodic Dipole Antenna*; Illinois Univ. at Urbana, Electrical Engineering Re-Search Lab: Champaign, IL, USA, 1961.

20. Carrel, R. The design of log-periodic dipole antennas. In Proceedings of the 1958 IRE International Convention Record, New York, NY, USA, 21–25 March 1966; Volume 9, pp. 61–75.
21. Duhamel, R.; Isbell, D. Broadband logarithmically periodic antenna structures. In Proceedings of the 1958 IRE International Convention Record, New York, NY, USA, 21–25 March 1966; Volume 5, pp. 119–128.
22. Campbell, C.; Traboulay, I.; Suthers, M.; Kneve, H.; Campbell, C.; Traboulay, I.; Suthers, M.; Kneve, H. Design of a stripline log-periodic dipole antenna. *IRE Trans. Antennas Propag.* **1977**, *25*, 718–721. [[CrossRef](#)]
23. Paul, A.; Gupta, I. An Analysis of Log Periodic Antenna with Printed Dipoles. *IEEE Trans. Microw. Theory Tech.* **1981**, *29*, 114–117. [[CrossRef](#)]
24. Pantoja, R.; Sapienza, A.; Filho, F. A microwave printed planar log-periodic dipole array antenna. *IRE Trans. Antennas Propag.* **1987**, *35*, 1176–1178. [[CrossRef](#)]
25. Kyei, A.; Sim, D.; Jung, Y. Compact log-periodic dipole array antenna with bandwidth-enhancement techniques for the low frequency band. *IET Microw. Antennas Propag.* **2017**, *11*, 711–717. [[CrossRef](#)]
26. Sun, Q.; Wang, J.; Cui, J.; Fu, J.; Zhou, C.; Wang, E. A compact printed log-periodic antenna with loaded stub. In Proceedings of the 2014 3rd Asia-Pacific Conference on Antennas and Propagation, Harbin, China, 26–29 July 2014; pp. 593–595.
27. Chen, J.; Ludwig, J.; Lim, S. Design of a Compact Log-Periodic Dipole Array Using T-Shaped Top Loadings. *IEEE Antennas Wirel. Propag. Lett.* **2017**, *16*, 1585–1588. [[CrossRef](#)]
28. Pirai, M.; RH, H. Size reduction of microstrip LPDA antenna with top loading. *IEICE Electron. Express* **2009**, *6*, 1528–1534. [[CrossRef](#)]
29. Anguera, J.; Puente, C.; Borja, C.; Soler, J. Fractal Shaped Antennas: A Review. In *Encyclopedia of RF and Microwave Engineering*; John Wiley & Sons, Inc.: Hoboken, NJ, USA, 2005.
30. Lalbakhsh, A.; Neyestanak, A.L.; Naser-Moghaddasi, M. Microstrip Hairpin Bandpass Filter Using Modified Min-kowski Fractal-Shape for Suppression of Second Harmonic. *IEICE Trans. Electron.* **2012**, *95*, 378–381. [[CrossRef](#)]
31. Lotfi-Neyestanak, A.; Lalbakhsh, A. Improved microstrip hairpin-line bandpass filters for spurious response suppression. *Electron. Lett.* **2012**, *48*, 858. [[CrossRef](#)]
32. Tripathi, S.; Mohan, A.; Yadav, S. A Compact UWB Koch Fractal Antenna for UWB Antenna Array Applications. *Wirel. Pers. Commun.* **2017**, *92*, 1423–1442. [[CrossRef](#)]
33. Oraizi, H.; Amini, A.; Mehr, M.K. Design of miniaturised UWB log-periodic end-fire antenna using several fractals with WLAN band-rejection. *IET Microw. Antennas Propag.* **2017**, *11*, 193–202. [[CrossRef](#)]
34. Gianvittorio, J.; Rahmat-Samii, Y. Fractal antennas: A novel antenna miniaturization technique, and applications. *IEEE Antennas Propag. Mag.* **2002**, *44*, 20–36. [[CrossRef](#)]
35. Anguera, J.; Puente, C.; Martínez, E.; Rozan, E. The fractal Hilbert monopole: A two-dimensional wire. *Microw. Opt. Technol. Lett.* **2002**, *36*, 102–104. [[CrossRef](#)]
36. Moallemzadeh, A.; Hassani, H.R.; Nezhad, S.M.A. Wide bandwidth and small size LPDA antenna. In Proceedings of the 2012 6th European Conference on Antennas and Propagation (EUCAP), Prague, Czech Republic, 26–30 March 2012; pp. 1–3.
37. Almalkawi, M.J.; Cross, L.W.; Alshamaileh, K.A. A transmission line circuit-oriented approach for miniaturization of a log-periodic dipole array (LPDA) antenna. In Proceedings of the 2014 IEEE 57th International Midwest Symposium on Circuits and Systems (MWSCAS), College Station, TX, USA, 3–6 August 2014; pp. 73–76. [[CrossRef](#)]
38. Gooran, P.R.; Lalbakhsh, A.; Moradi, H.; Jamshidi, M. (Behdad) Compact and wideband printed log-periodic dipole array antenna using multi-sigma and multi-Tau techniques. *J. Electromagn. Waves Appl.* **2019**, *33*, 697–706. [[CrossRef](#)]
39. Anagnostou, D.; Papapolymerou, J.; Tentzeris, M.M.; Christodoulou, C.G. A Printed Log-Periodic Koch-Dipole Array (LPKDA). *IEEE Antennas Wirel. Propag. Lett.* **2008**, *7*, 456–460. [[CrossRef](#)]
40. Rahman, N.; Jamlos, M. Miniaturized Log Periodic Fractal Koch Antenna with C-Shaped Stub. In Proceedings of the 2016 International Conference on Computer and Communication Engineering (ICCCCE), Kuala Lumpur, Malaysia, 26–27 July 2016; pp. 53–56.
41. Jain, S.K.; Shrivastava, A.; Shrivastava, G. Miniaturization of microstrip patch antenna using metamaterial loaded with SRR. In Proceedings of the 2015 International Conference on Electromagnetics in Advanced Applications (ICEAA), Turin, Italy, 7–11 September 2015; pp. 1224–1227.
42. Anim, K.; Jung, Y.-B. Shortened Log-Periodic Dipole Antenna Using Printed Dual-Band Dipole Elements. *IEEE Trans. Antennas Propag.* **2018**, *66*, 6762–6771. [[CrossRef](#)]
43. Khandelwal, M.K.; Kanaujia, B.; Gautam, A.K. Low Profile UWB Log-Periodic Dipole Antenna for Wireless Communication with Notched Band. *Microw. Opt. Technol. Lett.* **2013**, *55*, 2901–2906. [[CrossRef](#)]
44. Li, X.-R.; Ye, M.; Chu, Q.-X. Novel high gain printed log-periodic dipole antenna. In Proceedings of the 2016 IEEE International Symposium on Antennas and Propagation (APSURSI), Fajardo, PR, USA, 26 June–1 July 2016; pp. 1647–1648.
45. Chang, L.; He, S.; Zhang, J.Q.; Li, D. A Compact Dielectric-Loaded Log-Periodic Dipole Array (LPDA) Antenna. *IEEE Antennas Wirel. Propag. Lett.* **2017**, *16*, 2759–2762. [[CrossRef](#)]
46. Shin, G.; Kong, M.; Lee, S.-H.; Kim, S.-T.; Yoon, I.-J. Gain Characteristic Maintained, Miniaturized LPDA Antenna Using Partially Applied Folded Planar Helix Dipoles. *IEEE Access* **2018**, *6*, 25874–25880. [[CrossRef](#)]
47. Pantoja, M.F.; Bretones, A.C.R.; Ruiz, F.J.G.; Garcia, S.; Martin, R.G. Particle-Swarm Optimization in Antenna Design: Optimization of Log-Periodic Dipole Arrays. *IEEE Antennas Propag. Mag.* **2007**, *49*, 34–47. [[CrossRef](#)]

48. Golubovic, R.; Olcan, D. Antenna optimization using Particle Swarm Optimization algorithm. *J. Autom. Control.* **2006**, *16*, 21–24. [[CrossRef](#)]
49. Zaharis, Z.D.; Gravas, I.; Yioultsis, T.V.; Lazaridis, P.; Glover, I.A.; Skeberis, C.; Xenos, T.D. Exponential Log-Periodic Antenna Design Using Improved Particle Swarm Optimization With Velocity Mutation. *IEEE Trans. Magn.* **2017**, *53*, 1–4. [[CrossRef](#)]
50. Zaharis, Z.D.; Gravas, I.P.; Lazaridis, P.; Glover, I.A.; Antonopoulos, C.S.; Xenos, T.D. Optimal LTE-Protected LPDA Design for DVB-T Reception Using Particle Swarm Optimization With Velocity Mutation. *IEEE Trans. Antennas Propag.* **2018**, *66*, 3926–3935. [[CrossRef](#)]
51. Li, Y.; Yang, F.; Ouyang, J.; Zhou, H. Yagi-Uda Antenna Optimization Based on Invasive Weed Optimization Method. *Electromagnetics* **2011**, *31*, 571–577. [[CrossRef](#)]
52. Mallahzadeh, A.; Oraizi, H.; Davoodi-Rad, Z. Application of the invasive weed optimization technique for antenna configurations. *Prog. Electromagn. Res.* **2008**, *79*, 137–150. [[CrossRef](#)]
53. Pal, S.; Basak, A.; Das, S. Linear antenna array synthesis with modified invasive weed optimisation algorithm. *Int. J. Bio-Inspired Comput.* **2011**, *3*, 238. [[CrossRef](#)]
54. Sedighy, S.; Mallahzadeh, A.; Soleimani, M.; Rashed-Mohassel, J. Optimization of printed Yagi antenna using invasive weed optimization (IWO). *IEEE Antennas Wirel. Propag. Lett.* **2010**, *9*, 1275–1278. [[CrossRef](#)]
55. Lazaridis, P.I.; Tziris, E.N.; Zaharis, Z.D.; Xenos, T.D.; Cosmas, J.P.; Gallion, P.B.; Holmes, V.; Glover, I.A. Comparison of evolutionary algorithms for LPDA antenna optimization. *Radio Sci.* **2016**, *51*, 1377–1384. [[CrossRef](#)]